ELSEVIER

Biochimica et Biophysica Acta 1193 (1994) 118–126

BBA Biochimica et Biophysica Acta

Forces on biological cells due to applied alternating (AC) electric fields. I. Dielectrophoresis

Tohsak Lee Mahaworasilpa *, Hans G.L. Coster, Eric P. George

UNESCO Centre for Membrane Science and Technology, Department of Biophysics, University of New South Wales, P.O. Box 1, Kensington, N.S.W., Australia 2033

Received 8 February 1994

Abstract

Measurements are presented of dielectrophoretic forces for SP2 (mouse) and K562 (human) cells in external alternating electric fields over a frequency range of 10 kHz to 2 MHz. Using a spherical shell model of the cell, the dielectrophoretic force is derived from the interaction between the induced electric dipole moment in the cell and the external electric field. The frequency dependence of the force has its origin in the dispersion with frequency of the impedances of the cell membrane, the cytoplasm and the external medium (a Maxwell-Wagner dispersion). The predicted tri-phasic form of the variation of the dielectrophoretic force is in good agreement with the experimental results presented. Using the theoretical model, the experimental measurements also provided an estimation of 0.18 ± 0.03 S m^{-1} and 0.12 ± 0.04 S m^{-1} for the conductivities of the cytoplasm of cells of SP2 and K562, respectively, and 6.0 ± 2.0 mF m^{-2} and 2.0 ± 1.0 mF m^{-2} for the capacitances of the plasma membrane of these cells.

Key words: Dielectrophoresis; Cell electro-dynamics; Cell membrane; Membrane capacitance; Induced electric dipole

1. Introduction

Interactions of particles and biological cells with electric fields have been the subject of many investigations [1–6,22]. When a biological cell is suspended in a poorly conducting medium in an AC electric field, an electric dipole is induced in the cell. If the applied field is non-uniform, the interaction between the field and the induced dipole moment leads to a net translational force, the so called 'dielectrophoretic' (DEP) force [4–11,22]. Many investigators have observed dielectrophoresis of biological cells in non-uniform electric fields [3,7–9,12–15]. The DEP force may be calculated from the electric energy and momentum balance [6,22] of a dielectric particle suspended in a lossy dielectric medium. Pohl [3] obtained an expression for the dielectrophoretic force on cells suspended in a medium by modelling the cell as a solid spherical dielectric particle with a complex permittivity ϵ'_c suspended in an external medium with a complex permittivity ϵ'_s. A more realistic dielectric model for a biological cell consists of a spherical dielectric shell and this model has been adopted by a number of investigators (e.g., [6,7,11,22]). This model allows one to account specifically for the dielectric properties of the plasma membrane (shell) and the cytoplasm. The calculation of the DEP can be somewhat simplified by replacing the spherical particle, complete with the dielectric shell, with an equivalent homogeneous single phase dielectric particle with an effective (complex) permittivity ϵ'_{eff} [11].

The expression for the DEP force of the spherical cell model in an external AC electric field, $\boldsymbol{E}$, is then given by [6,11]:

$$\boldsymbol{F}_{DEP} = 2\pi\epsilon_s R^3 \,\mathrm{Re}\left[\frac{(\epsilon'_{eff} - \epsilon'_s)}{(\epsilon'_{eff} + 2\epsilon'_s)}\right]\nabla(E^2) \qquad (1)$$

where $\epsilon'_s = \epsilon_s - j\sigma_s/\omega$ is the complex permittivity of the suspending medium with a permittivity ϵ_s and conduc-

* Corresponding author. Fax: (61) 02-663-3420.

SSDI 0005-2736(94)00040-V

tivity of σ_s, ϵ'_{eff} is the effective complex permittivity of the cell membrane and cytoplasm; the expression for which has been derived elsewhere [11] and ω is the angular frequency of the electric field, R is the radius of cell.

In Eq. (1), the quantity

$$\mathrm{Re}\left[\frac{\epsilon'_{eff}-\epsilon'_s}{\epsilon'_{eff}+2\epsilon'_s}\right]=\mathrm{Re}[f(\omega)]$$

is the real part of a complex function $f(\omega)$ which varies with frequency (see also the Appendix).

In terms of the induced dipole moment, which will be frequency dependent (see the Appendix), the DEP force is given by

$$F_{DEP}=\mathrm{Re}[(\mu(\omega)\nabla)E] \quad (2)$$

where the induced dipole moment $\mu(\omega)$ is given by

$$\mu(\omega)=4\pi\epsilon_s R^3 f(\omega)E \quad (3)$$

and hence

$$F_{DEP}=2\pi\epsilon_s R^3\,\mathrm{Re}[f(\omega)]\nabla(E^2) \quad (4)$$

The function $\mathrm{Re}[f(\omega)]$ and its explicit dependence on frequency and the dielectric and conductance parameters of the model is given in the Appendix.

We describe here measurements of the dielectrophoretic force on *single* cells of SP2 (mouse) and K562 (human) cell lines in AC electric fields produced between a pair of parallel cylindrical (wire) electrodes. The SP2 cell line has frequently been employed as a fusion partner cell for mouse hybridoma production. The K562 cell line is a well established cell line used in many cell biology laboratories. The study of electrotranslation is relevant to the manipulation of cells in general and in particular as a means of bringing two or more cells into good contact for the purpose of electrically inducing cell fusion.

2. Materials and methods

The cell lines SP2 and K562 were obtained directly from the American Type Culture Collection (ATCC). Both cell lines were cultured in RPMI + 10% FCS and passaged every 3 days. The cells in the logarithmic phase of their growth were used for the measurements. For each specimen, the cells were washed twice in 100 mM sorbitol by centrifugation at $100\times g$ for 5 min, removing the supernatant and resuspending the pellet of cells in the wash medium. New batches of washed cells were prepared and used within 15 min after cell wash. The radius of the cell, R, was measured optically in each experiment.

The dielectrophoretic force acting on a cell was

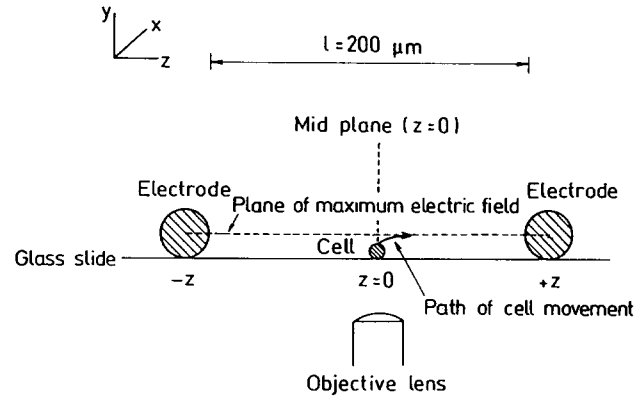

Fig. 1. Cross-sectional view (not to scale) of the cell arrangement in the cell chamber for the dielectrophoresis study.

determined by the following method. When a cell of radius R translates under the influence of an electric field which is directed in a horizontal plane [1] in a medium with a viscosity η, the horizontal dielectrophoretic force on the cell (F_{DEP}) is counter-balanced by the Stokes' drag force F_η, where $F_\eta = -6\pi\eta R v$. The drift velocity in the horizontal direction therefore provides a direct measure of the DEP force acting on the cell. From the expression for F_{DEP} given by Eq. (4), one obtains

$$6\pi\eta R v=2\pi\epsilon_s R^3\,\mathrm{Re}[f(\omega)]\nabla(E^2) \quad (5)$$

or

$$v=\frac{\epsilon_s R^2\,\mathrm{Re}[f(\omega)]\nabla(E^2)}{3\eta} \quad (6)$$

The horizontal drift velocity in the field is therefore predicted to be proportional to the gradient in E^2. Measurements of v as a function of $\nabla(E^2)$ allow us to estimate the magnitude of $\mathrm{Re}[f(\omega)]$ which depends on the dielectric properties and conductivities of the external medium, the cytoplasm and the cell membrane, the specific capacitance of the cell membrane, as well as the frequency of the electric field (see Appendix).

The measurements of velocity (and hence force) were made in a glass-bottom chamber consisting of a circular well in a perspex block. Two uncoated nickel alloy cylindrical wires (128 μm in diameter) were used as the electrodes. Both electrodes were mounted on micromanipulators (Narishige Scientific) in such a way that the electrodes were oriented parallel to each other. A single cell could be placed at any location between the electrodes; although the preferred position was

[1] By restricting ourselves to movement in the horizontal direction, we avoid problems associated with the vertical force exerted on the cell by gravity.

close to the midpoint between the electrodes, i.e., $z = 0$ (Fig. 1). The spacing, l, between the surfaces of the electrodes in the equatorial plane was kept constant at 200 μm throughout the experiments (Fig. 1).

Using cylindrical (wire) electrodes, the electric field (E) in the z direction between two, long, cylindrical wire electrodes to which a potential difference (V) is applied, varies with position and is given by:

$$E(z) = \frac{Vd}{\left[2\ln\left(\frac{d-a}{a}\right)\right]\left[\frac{d^2}{4} - z^2\right]} \quad (7)$$

where a is the radius of each electrode, d is the parallel electrode separation with respect to their centres and ln is the natural logarithm.

For example, the external field strengths (E) and $\nabla(E^2)$ versus z (in the equatorial plane) between a pair of parallel, cylindrical electrodes for two applied voltages across the electrodes are given in Fig. 2a and 2b.

The field strength midway between the electrodes ($z = 0$) in the vertical direction is given by

$$E(y) = \frac{Vd}{\left[2\ln\left(\frac{d-a}{a}\right)\right]\left[\frac{d^2}{4} + y^2\right]} \quad (8)$$

where y is the distance in the vertical direction from the equatorial plane. The variation of E with y at $z = 0$ is shown in Fig. 2c.

Measurements of cell movements in non-uniform electric fields were made on (*single*) cells isolated from other cells so that there were no cell-to-cell interactions. To achieve this, the cell was positioned at $z = 0$ (Fig. 1) and at rest in the bottom of the chamber. An AC voltage with a known amplitude at a given frequency was then applied across the electrodes. The applied voltage caused the cell to be raised from the bottom of the chamber to the equatorial plane where the electric field was maximum (see Fig. 2c). The cell was also ultimately attracted towards either electrode. Only the portion of the cell movement in the plane of maximum electric field (equatorial plane) was recorded and used for analysis.

All measurements were carried out using an optical/video-recording system which consisted of an inverted microscope (Nikon 'Diaphot') fitted with Differential Interference Contrast optics, a colour video camera, a video cassette recorder and a colour TV monitor. The translational velocity of the cell could be

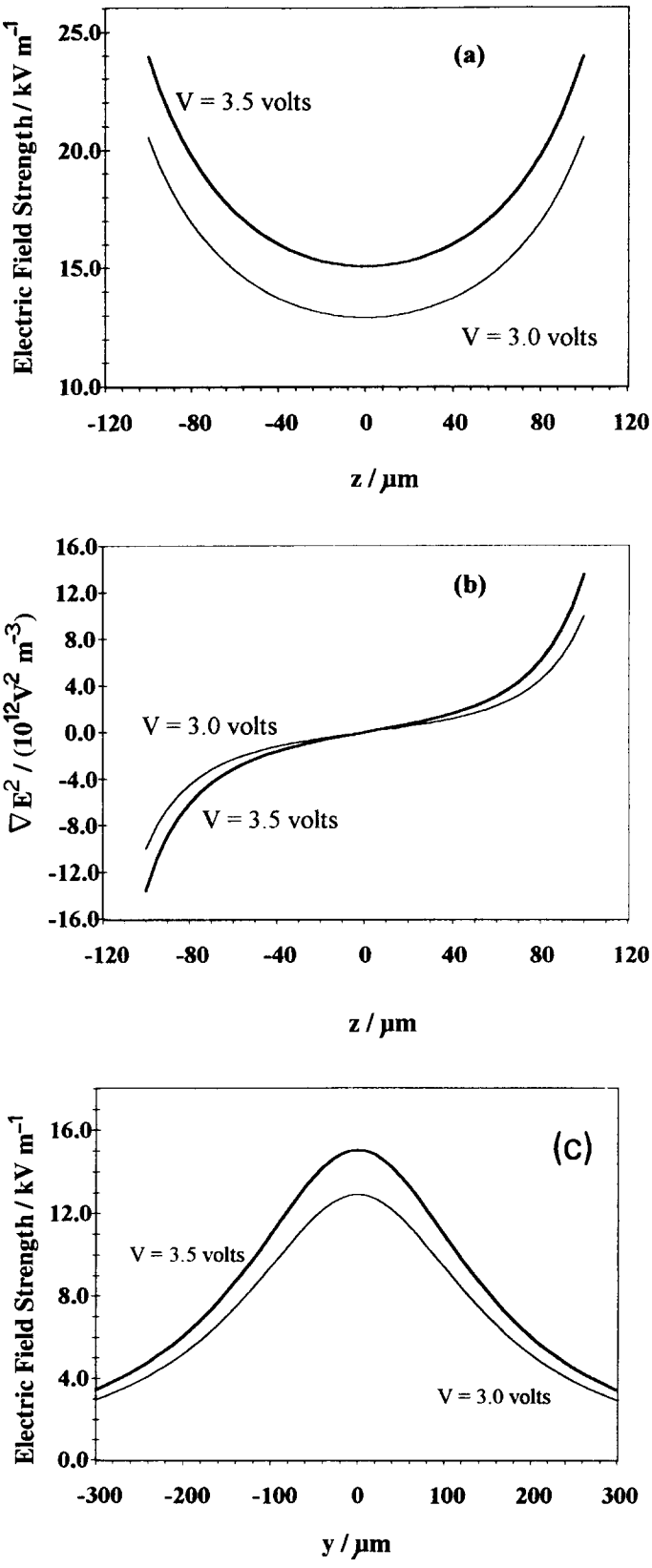

Fig. 2. (a) Electric field profiles in the space (z) between a pair of parallel electrodes (in the equatorial plane). (b) Their gradients in E^2 as a function of position (z) between the electrodes (in the equatorial plane). (c) Electric filed strengths midway between the electrodes ($z = 0$) as a function of position (y) in the vertical direction from the equatorial plane (see also Fig. 1 for the axes) for $a = 64$ μm, $d = 328$ μm and $l = 200$ μm (where a, d and l are defined in text).

determined from an analysis of the video recording on a frame by frame basis. This provides a time resolution of 40 ms (25 frames per second in the Australian PAL video protocols).

To reduce errors in the cell translation measurements, the video-optical system was set up such that the focal plane of the image was in the plane of maximum electric field. For field frequencies where the dielectrophoretic force was negative (low and very high frequencies), the cell moves out of the equatorial plane and its movement is not confined to a plane. This makes it essentially impossible to track its movement quantitatively using the microscope. Our experimental method is therefore restricted to the frequency range where the dielectrophoretic force is positive (when the cell moves towards regions of stronger field) which keeps the cell in the equatorial plane and moves it towards one of the electrodes in that plane.

The viscosity of 100 mM sorbitol solution was measured at 25°C using an Oswald U-tube viscometer and found to be $(1.05 \pm 0.03) \times 10^{-3}$ N s m^{-2}.

Video re-plays of the recorded movements of a cell on a frame by frame basis allowed the time, t, and the displacements, z, of the cell to be measured. A plot of displacement versus time for a given frequency and electric field strength was made and a smooth curve was fitted to the experimental data of displacement at different times to allow the velocity to be determined as a function of displacement. Cells reached a terminal drift velocity in times very short compared to the frame rate of the video camera and hence changes in velocity directly reflected changes in the driving force (i.e., dielectrophoresis) acting on the cell. The whole process was repeated for a number of cells and for various AC field frequencies.

3. Results

Plots of the experimental data of $3\eta v/\epsilon_s R^2$ against $\nabla(E^2)$ for various AC frequencies for SP2 cells are shown in Fig. 3. These results suggest a linear relation-

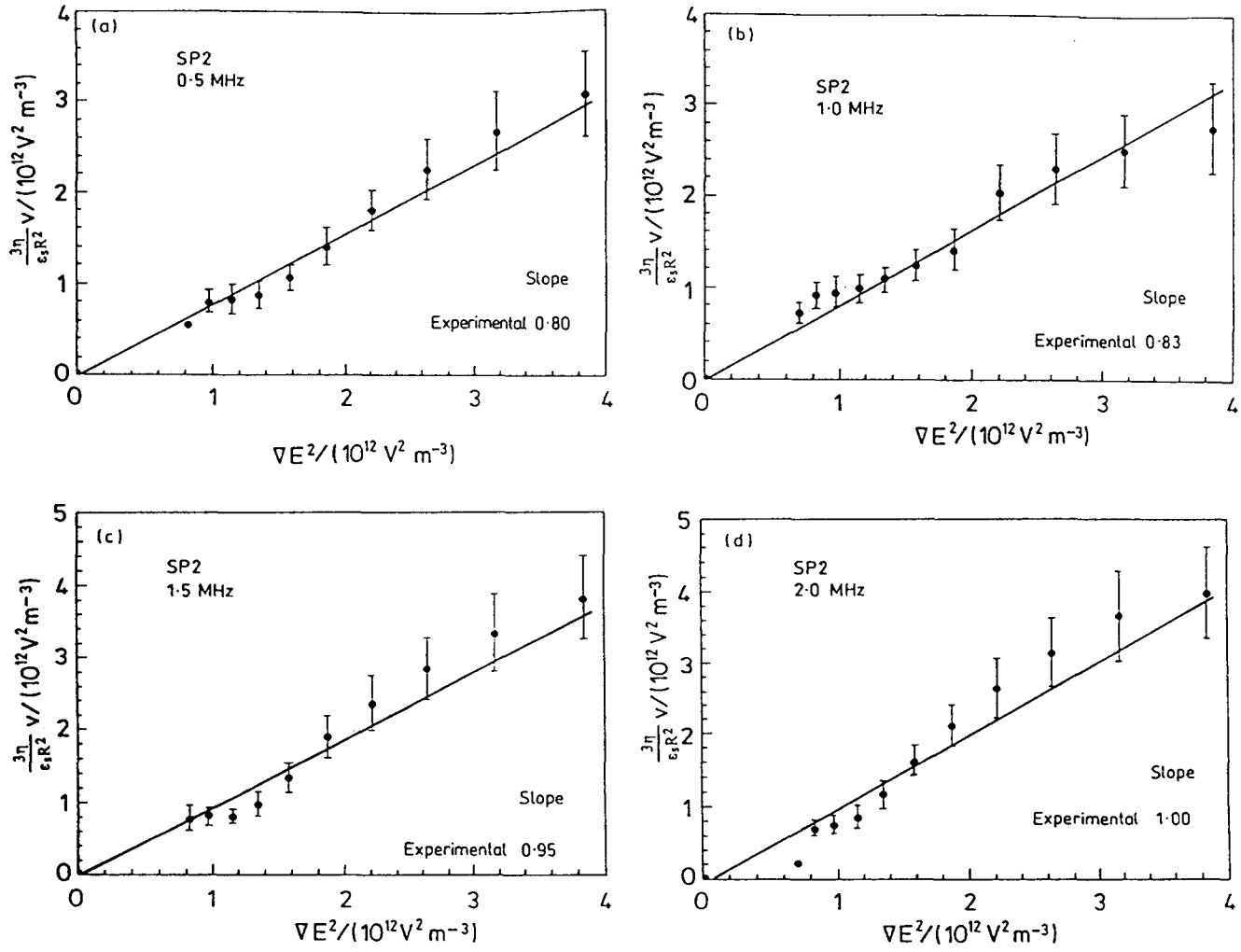

Fig. 3. Experimental plots of $3\eta/\epsilon_s R^2 v$ as a function of ∇E^2 for SP2 cells suspended in 100 mM sorbitol and for various field frequencies (e.g., 0.5 to 2.0 MHz). The slope of each linear regression line for a given frequency is also indicated.

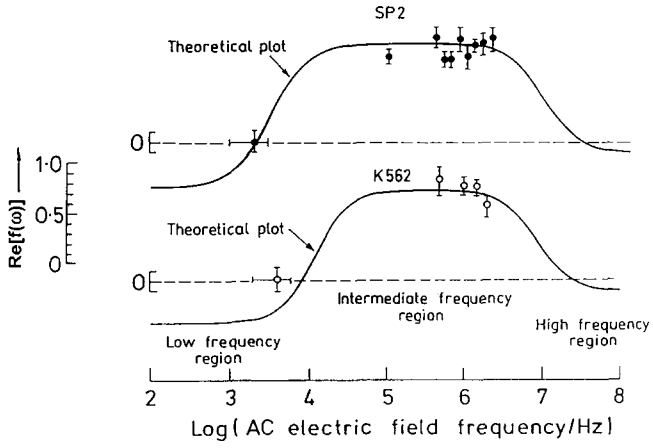

Fig. 4. Plots of theoretical (———) and experimental values (•) of Re[$f(\omega)$] versus field frequency for SP2 and K562 cells. The average values of Re[$f(\omega)$] for a frequency range of 0.3 to 2.0 MHz for SP2 and K562 cells were found to be 0.95 ± 0.14 and 0.89 ± 0.10, respectively.

ship between $3\eta v/\epsilon_s R^2$ and $\nabla(E^2)$ as predicted by Eq. (6). Similar results (not shown here) were also obtained for K562 cells. A linear regression analysis indicates that the mean correlation coefficient for the lines plotted was in the range of 0.88 to 0.95. The slope of the regression line was used to determine Re[$f(\omega)$]. Re[$f(\omega)$] was determined in this manner from experimental results obtained at a number of field frequencies. Plots of Re[$f(\omega)$] determined from these experiments, as a function of field frequency, for SP2 and K562 cells are shown in Fig. 4. Over the frequency range 0.3 MHz to 2 MHz, Re[$f(\omega)$] was found to be largely *frequency independent*, with an average value of 0.95 ± 0.14 (S.D.) for SP2 and 0.89 ± 0.10 (S.D.) for K562. The line plotted in Fig. 4 is a plot of the theoretical variation of Re[$f(\omega)$] (Eq. (A-13) in the Appendix) with frequency obtained by adjusting the relevant parameters to attain the best fit to the data over the *whole* frequency range used in the experiments and not just the frequencies at which the force was zero.

4. Discussion

The dielectrophoretic spectrum of Re[$f(\omega)$] versus frequency is affected by the choice of the dielectric and conductance parameters of the spherical shell model used in the analysis. Different parameters generally affect different characteristic features of the spectrum. Some examples of this are shown in Figs. 5a–5f, in which in each instance one parameter is varied while holding the other parameters constant. Dramatic effects are seen in the effect of the conductivity of the external medium (σ_s), the conductivity of the cytoplasm (σ_c) and the conductivity of the plasma membrane (σ_m). Thus increasing σ_s shifts the cross over point from negative to positive dielectrophoresis to higher frequencies while this does not affect the high frequency cross over point and only marginally affects the

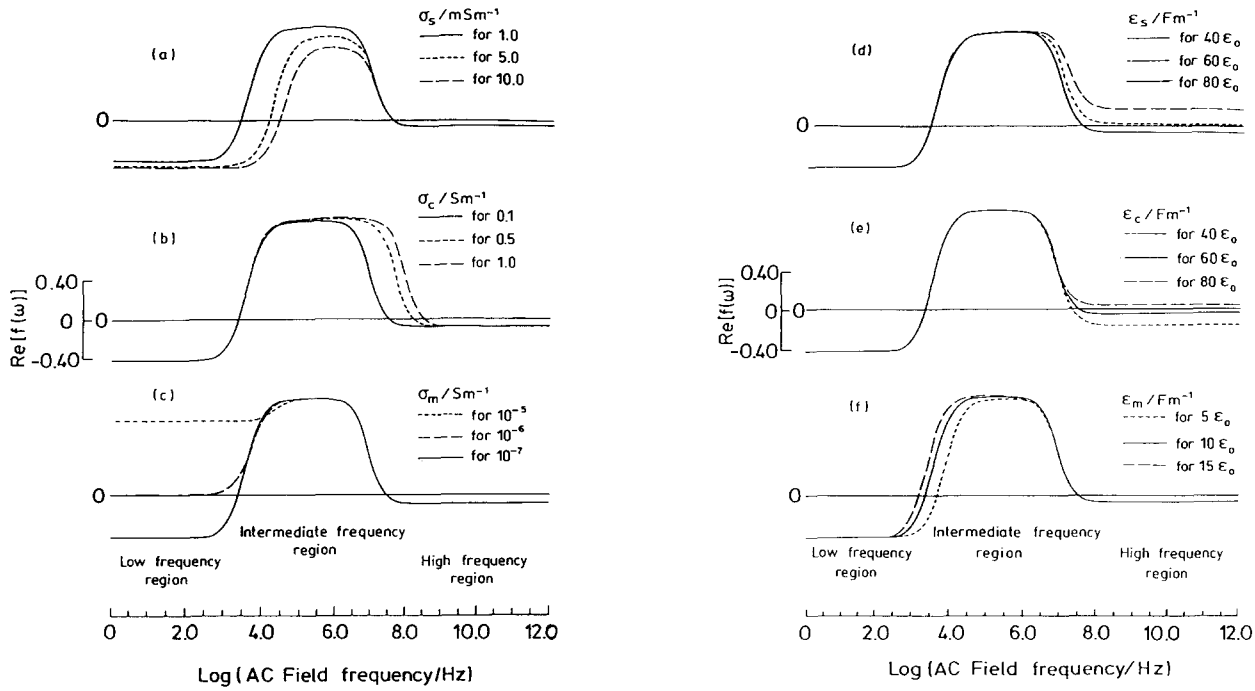

Fig. 5. Theoretical plots of Re[$f(\omega)$] as a function of field frequency for various values of the conductivities (a, b and c) and permittivities (d, e and f) of the external medium, the cytoplasm and the cell membrane, respectively. The solid lines were plotted using the following parameters: $\sigma_s = 0.001$ S m^{-1}, $\sigma_c = 0.1$ S m^{-1}, $\sigma_m = 10^{-7}$ S m^{-1}, $\epsilon_s = 80\ \epsilon_0$, $\epsilon_c = 60\ \epsilon_0$, $\epsilon_m = 10\epsilon_0$, $R = 10\ \mu$m and $\delta = 10$ nm.

maximum value of the positive dielectrophoresis in the mid frequency range. In contrast, σ_c affects the high frequency cross over frequency at which the positive DEP changes over to negative DEP. This parameter does not affect the low frequency cross over point, nor the maximum value of the positive DEP in the mid frequency range. The value of the conductance of the membrane (σ_m) does not affect the cross over frequencies but has a dramatic effect on the strength of the negative DEP at low frequencies; at sufficiently high values of σ_m, the negative DEP in the low frequency region is abolished and only positive DEP occurs. The cross over point to negative DEP at high frequencies is not affected by this parameter.

The values of the dielectric constant of the external medium (ϵ_s), the cytoplasm (ϵ_c) and the membrane (ϵ_m) also affect on the DEP spectrum. Decreasing values of ϵ_s shift the high frequency cross over point to higher frequencies and decrease the negative DEP in the high frequency region; at sufficiently low value of ϵ_s the DEP force at high frequencies is always positive. The value of ϵ_c affects the magnitude of the high frequency DEP (making it more positive as ϵ_c increases) but does not affect the frequency of the high frequency cross over point. The value of ϵ_m only affects the frequency of the low frequency cross over point but does not affect the magnitude of either the negative DEP at low frequencies or the positive DEP at the mid frequency range. It has no effect on the high frequency region. The zero-crossing point of Re[$f(\omega)$] as a function of frequency is thus most sensitive to variations in the dielectric and conductance properties of the cell cytoplasm, membrane and the medium whilst the *magnitude* of Re[$f(\omega)$] at low frequencies is most sensitive to the conductance of the membrane. A detailed theoretical analysis of the sensitivity of the profile of Re[$f(\omega)$] on the complex dielectric parameters has also been presented by Foster et al. [10].

The calculation of the theoretical DEP force for our dielectric shell model of the cell is valid only if the non-uniformity of the field $\boldsymbol{E}$ is low. When the field $\boldsymbol{E}$ is highly non-uniform, higher order moments are generated and this could result in significant errors in the calculation of the DEP force [15–17]. On the other hand Jones [17] found that the higher order moments were insignificant if the size of the object (e.g., a cell) in the field was much less than the dimension of the electrodes. This is the case for the present study where the diameters of SP2 and K562 cells suspended in 100 mM sorbitol solution ($\sim$ 15–20 μm) are much less than the diameters of the electrodes (128 μm).

Since the measurements were made in the equatorial plane of the electrodes (where the field was maximum) which was far away from the bottom of the chamber (i.e., the distance was $\sim$ 64 μm comparing to the radius of the cell which was $\sim$ 10 μm) and the field distribution in the vertical plane (perpendicular to the equatorial plane) decreased rapidly, the effect of the interface between the external solution and the glass at the bottom of the chamber on the electric field profile can be considered insignificant.

The force measurements in the present investigation were based on the assumption that the cell being observed was a small dielectric *spherical* shell. Biological cells in an intense electric field also undergo deformation and during the measurements cell deformation did take place, particularly as the cell migrated close towards one of the electrodes. The deformation of the cell would alter the electric field profile from that assumed in the analysis as well as altering the calculation of the viscous retardation force using the Stokes' equation. To minimise these possible sources of complication, only the motion of the cells in the regions of lower field strength (far away from the electrodes) was included in the analysis presented. Despite these possible complications, the experimental results agreed well with the theoretical prediction given in Eq. (3). The dielectrophoresis for intermediate frequencies (0.3 to 2 MHz) was found to be independent of the frequency of the applied electric field, as predicted by the form of Re[$f(\omega)$] (cf. Fig. A-2).

Fitting the theoretical curve for Re[$f(\omega)$] as a function of frequency to the experimental data points (Fig. 4) yielded the dielectric and conductance values shown in Table 1 for cells of SP2 and K562. In the calculations it was assumed that the external solution (100 mM sorbitol) had a dielectric constant (ϵ_s) of $78\epsilon_0$. For the calculation of ϵ_m it was assumed that the membrane thickness was 10 nm; the conductance of the membrane was assumed negligible. The conductivity of the 100 mM sorbitol solution was measured independently and was found to be 1.0 ± 0.2 mS m^{-1}.

These estimated values of the conductances of the cytoplasm for SP2 and K562 (0.18 ± 0.03 S m^{-1} and 0.12 ± 0.04 S m^{-1}, respectively) are below the most frequently quoted values for animal erythrocytes (i.e., 0.4 to 0.8 S m^{-1} [18,19]). This may be due to the fact

Table 1
Summary of the conductivities and permittivities of the external medium, the cytoplasm and the cell membrane for SP2 and K562 cells

Parameters	SP2 cells	K562 cells
σ_s (mS m^{-1}) [a]	1.0 ± 0.2	1.0 ± 0.2
σ_c (S m^{-1}) [b]	0.18 ± 0.03	0.12 ± 0.04
σ_m (S m^{-1}) [c]	10^{-7}	10^{-7}
ϵ_s [c]	$78\ \epsilon_0$	$78\ \epsilon_0$
ϵ_c [c]	$60\ \epsilon_0$	$60\ \epsilon_0$
ϵ_m [b]	$11\ \epsilon_0$	$3\ \epsilon_0$
C_m (mF m^{-2}) [b]	6.0 ± 2.0	2.0 ± 1.0

The membrane capacitances (C_m) for both cell types are also shown.
[a] Measured values; [b] estimated values; [c] assumed values.

that the commonly published values were obtained using cells suspended in isotonic solutions, whereas the cells in the present study were suspended in a hypotonic solution (100 mM sorbitol has an osmolality of ~ 100 mosmol kg^{-1}). This could affect the conductivity of the cytoplasm because in the sorbitol solution the cells were swollen by an osmotic uptake of water (the volume of the cells increased by a factor of approximately 3). This was done to ensure that the cells were close to spherical in shape. It would be of interest to repeat these measurements as a function of the degree of swelling of the cells.

The specific membrane capacitances for SP2 and K562 cells were estimated to be 6.0 ± 2.0 mF m^{-2} and 2.0 ± 1.0 mF m^{-2}, respectively. While these values fall in the range reported in the literature for mammalian cells, the lower value, 2.0 ± 1.0 mF m^{-2} for K562 cells, is lower than the frequently quoted values for living cells (e.g., 8 to 13 mF m^{-2} for mammalian cells [19,20] and 5 to 15 mF m^{-2} for plant cells [11,21]). It is not clear whether this is a feature of cancer cell lines in general or indicates that additional features such as the nucleus of the cell (and nuclear membrane) should be taken into account [24].

Appendix

The induced dipole moment, μ, for a homogeneous spherical, non-conducting particle with a complex permittivity ϵ'_p in a non-conducting medium of a complex permittivity ϵ'_s and in an AC electric field **E** with an angular frequency ω is given by

$$\mu(\omega) = 4\pi R^3 \epsilon_s \left[\frac{\epsilon'_p - \epsilon'_s}{\epsilon'_p + 2\epsilon'_s}\right] E \qquad \text{(A-1)}$$

For an inhomogeneous spherical particle (Fig. A-1) with a dielectric shell with a complex permittivity ϵ'_m and a complex conductivity σ'_m enclosing a conducting interior with a complex permittivity ϵ'_c and a complex conductivity σ'_c, Maxwell [23] showed that at a given electric field frequency this shell model can be replaced by an equivalent homogeneous sphere with an effective complex conductivity σ'_{eff} which is given by

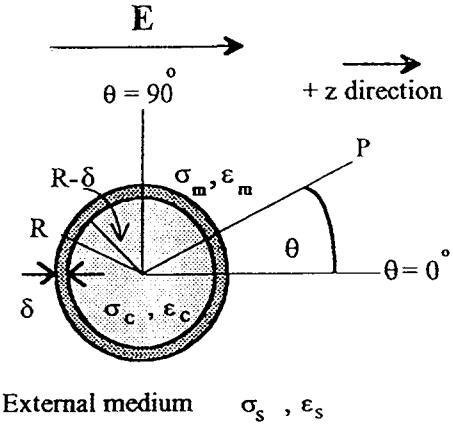

Fig. A-1. Spherical dielectric shell model for a mammalian cell. δ is the thickness of the shell (the cell membrane), R is the outer radius of the shell. ϵ_m, ϵ_c and ϵ_s are the permittivities of the membrane, the cytoplasm and the external medium, respectively. σ_m, σ_c and σ_s are the conductivities of the membrane, the cytoplasm and the external medium, respectively.

$$\sigma'_{eff} = -\frac{\sigma'_m\left[2(R-\delta)^3(\sigma'_c - \sigma'_m) + R^3(\sigma'_c + 2\sigma'_m)\right]}{\left[(R-\delta)^3(\sigma'_c - \sigma'_m) - R^3(\sigma'_c + 2\sigma'_m)\right]} \qquad \text{(A-2)}$$

Since $\sigma' = j\omega\epsilon'$ (where ω is the angular frequency of the electric field), Eq. (A-2) can then be written as

$$\epsilon'_{eff} = -\frac{\epsilon'_m\left[2(R-\delta)^3(\epsilon'_c - \epsilon'_m) + R^3(\epsilon'_c + 2\epsilon'_m)\right]}{\left[(R-\delta)^3(\epsilon'_c - \epsilon'_m) - R^3(\epsilon'_c + 2\epsilon'_m)\right]} \qquad \text{(A-3)}$$

The induced dipole moment $\mu(\omega)$ in the dielectric-shell sphere when suspended in a liquid medium with a complex conductivity σ'_s and a complex permittivity ϵ'_s is then given by [4,6,11]

$$\mu(\omega) = 4\pi R^3 \epsilon_s \left[\frac{\epsilon'_{eff} - \epsilon'_s}{\epsilon'_{eff} + 2\epsilon'_s}\right] E \qquad \text{(A-4)}$$

$$= 4\pi R^3 \epsilon_s f(\omega) E \qquad \text{(A-5)}$$

where we have defined the complex, frequency dependent, function $f(\omega)$ as:

$$f(\omega) = \left[\frac{\epsilon'_{eff} - \epsilon'_s}{\epsilon'_{eff} + 2\epsilon'_s}\right] \qquad \text{(A-6)}$$

$$= -\frac{(1-\alpha_s)(1+2\alpha_c) - (1+2\alpha_s)(1-\alpha_c)\left(\frac{R-\delta}{R}\right)^3}{(2+\alpha_s)(1+2\alpha_c) - 2(1-\alpha_s)(1-\alpha_c)\left(\frac{R-\delta}{R}\right)^3} \qquad \text{(A-7)}$$

where

$$\alpha_s = \frac{\epsilon'_m}{\epsilon'_s} = \frac{\sigma_m + j\omega\epsilon_m}{\sigma_s + j\omega\epsilon_s} \qquad \text{(A-8)}$$

and

$$\alpha_c = \frac{\epsilon'_m}{\epsilon'_c} = \frac{\sigma_m + j\omega\epsilon_m}{\sigma_c + j\omega\epsilon_c} \qquad \text{(A-9)}$$

(R = radius of the cell, δ = thickness of the membrane (shell)).

For mammalian cells, the ratio of the thickness of the membrane (shell) to the radius of the cell (δ/R) is typically as small as 10^{-3}. Hence $f(\omega)$ can be simplified to

$$f(\omega) = -\frac{(\alpha_c - \alpha_s) + (1+2\alpha_s)(1-\alpha_c)\frac{\delta}{R}}{(\alpha_s + 2\alpha_c) + (1-\alpha_s)(1-\alpha_c)\frac{2\delta}{R}} \qquad \text{(A-10)}$$

The interaction between the applied electric field **E** and the induced dipole μ produces a dielectrophoretic force acting on the cell which is given by:

$$F_{DEP} = \mathrm{Re}[(\mu(\omega)\cdot\nabla)E]$$
$$= 2\pi\epsilon_s R^3 \nabla(E^2)\,\mathrm{Re}[f(\omega)] \qquad \text{(A-11)}$$

where $\mathrm{Re}[f(\omega)]$ is the real part of the complex function $f(\omega)$.

The explicit calculation of $f(\omega)$ and hence the dipole moment is somewhat tedious. Briefly, it is necessary to determine the potential distribution by solution of the Laplace equations for the field, using the condition of continuity of the normal components of $D = \epsilon E$ and the tangential components of E at the interfaces of the various dielectrics. The dipole moment can then be deduced by comparison of the expression of the potential as a function of radial position, r, and azimuth angle, θ, with the potential ψ_μ as a function of position of a dipole:

$$\psi_\mu = \frac{\mu\cos\theta}{4\pi\epsilon_s r^2} \qquad \text{(A-12)}$$

This then yields ultimately an expression for $\mathrm{Re}[f(\omega)]$ as follows:

$$\mathrm{Re}[f(\omega)] = -\left[\frac{AB + CD\omega^2}{B^2 + D^2\omega^2}\right] \qquad \text{(A-13)}$$

where:

$$A = (2k-1)(\sigma_c\sigma_m - \epsilon_c\epsilon_m\omega^2) + (1-k)(\sigma_s\sigma_m - \epsilon_s\epsilon_m\omega^2) + k[\sigma_s\sigma_c - 2\sigma_m^2 + \omega^2(2\epsilon_m^2 - \epsilon_s\epsilon_c)]$$

$$B = (1-2k)(\sigma_c\sigma_m - \epsilon_c\epsilon_m\omega^2) + 2(1-k)(\sigma_s\sigma_m - \epsilon_s\epsilon_m\omega^2) + 2k[\sigma_s\sigma_c + \sigma_m^2 - \omega^2(\epsilon_m^2 + \epsilon_s\epsilon_c)]$$

$$C = (2k-1)(\sigma_m\epsilon_c + \sigma_c\epsilon_m) + (1-k)(\sigma_m\epsilon_s + \sigma_s\epsilon_m) + k(\sigma_c\epsilon_s + \sigma_s\epsilon_c - 4\sigma_m\epsilon_m)$$

$$D = (1-2k)(\sigma_m\epsilon_c + \sigma_c\epsilon_m) + 2(1-k)(\sigma_m\epsilon_s + \sigma_s\epsilon_m) + 2k(\sigma_c\epsilon_s + \sigma_s\epsilon_c + 2\sigma_m\epsilon_m)$$

and $k = \delta/R$

Fig. A-2 shows a theoretical plot of both the real and imaginary components of $f(\omega)$ as a function of applied electric field frequency. A similar plot for $\mathrm{Re}[f(\omega)]$ has been presented elsewhere [11]. The interfacial polarisation effects which lead to the frequency dependence of the induced electric dipole in the cell is illustrated in Fig. A-3; in this instance for the situation where $\epsilon_c < \epsilon_s$. The most important features to note are: (a) in the low and very high field frequency regions, μ is in the opposite direction to the applied electric field E, whereas in the intermediate frequency region μ is in the same direction as the applied electric field and (b) the magnitudes of the dipole in the low and very high frequencies are smaller than that in the intermediate frequency region. Note that the dielectrophoretic force acting on the cell causes the cell to migrate towards regions of higher electric filed

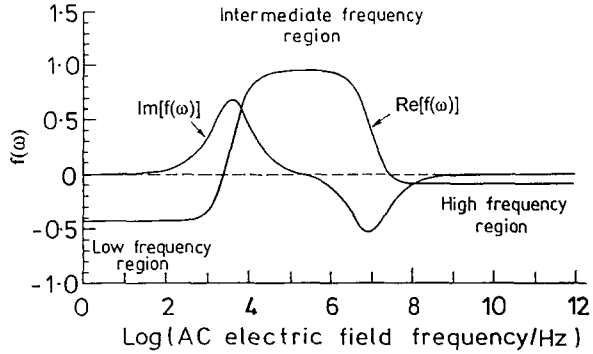

Fig. A-2. Theoretical plots of $\mathrm{Re}[f(\omega)]$ and $\mathrm{Im}[f(\omega)]$ versus logarithm of field frequency for the following parameters: $\sigma_s = 0.001$ Sm^{-1}, $\sigma_c = 0.1$ Sm^{-1}, $\sigma_m = 10^{-7}$ Sm^{-1}, $\epsilon_s = 78$ ϵ_0, $\epsilon_c = 60$ ϵ_0, $\epsilon_m = 10$ ϵ_0. Radius of cell $(R) = 10$ μm and thickness of the cell membrane $(\delta) = 10$ nm (where ϵ_0 is the permittivity of the free space $= 8.85\times10^{-12}$ Fm^{-1}).

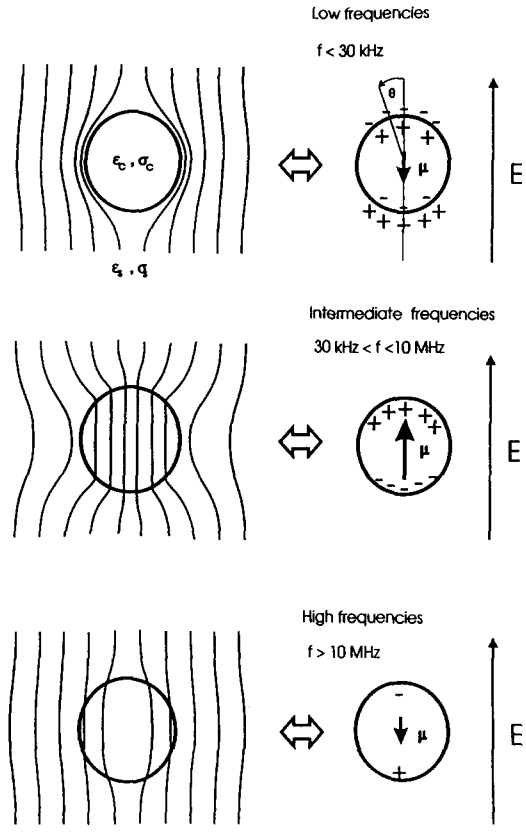

Fig. A-3. Diagrams showing applied electric field lines and the corresponding equivalent induced dipoles in a dielectric shell sphere when it is suspended in a poorly conducting medium and in an electric field of low, intermediate and high frequency. In the example $\epsilon_c < \epsilon_s$ and $\sigma_c > \sigma_s$ while $\sigma_m \ll \sigma_c$.

strengths when Re[$f(\omega)$] is positive and to move away from higher field strengths when Re[$f(\omega)$] is negative.

Acknowledgments

The authors wish to acknowledge the support of the Australian Research Council and the UNESCO Centre for Membrane Science and Technology. The award of a postgraduate scholarship to TLM from the University of New South Wales is also gratefully acknowledged.

References

[1] Coster, H.G.L. and Zimmermann, U. (1975) Biochim. Biophys. Acta 382, 410–418.
[2] Coster, H.G.L. and Zimmermann, U. (1975) J. Membr. Biol. 22, 73–90.
[3] Pohl, H.A. (1978) in Dieletrophoresis, Cambridge University Press, London.
[4] Sauer, F.A. and Schlogl, R.W. (1985) in Interactions between Electromagnetic Fields and Cells (Chiabrere, A., Nicolini, C. and Schwan, H.P., eds.), pp. 203–251, Plenum Press, New York.
[5] Jones, T.B. and Bliss, G.W. (1977) J. Appl. Phys. 48, 1412–1417.
[6] Sauer, F.A. in (1985) in Interactions between Electromagnetic Fields and Cells (Chiabrere, A., Nicolini, C. and Schwan, H.P. eds.), pp. 181–202, Plenum Press, New York.
[7] Marszalek, P., Zielinski, J.J. and Fikus, M. (1989) Bioelectrochem. Bioenerg. 22, 289–298.
[8] Dimitrov, D.S., Apostolova, M.A. and Sowers, A.E. (1990) Biochim. Biophys. Acta 1023, 389–397.
[9] Burt, J.P.H., Pethig, R., Gascoyne, P.R.C. and Becker, F.F. (1990) Biochim. Biophys. Acta 1034, 93–101.
[10] Foster, K.R., Sauer, F.A. and Schwan, H.P. (1992) Biophys. J. 63, 180–190.
[11] Kaler, K.V.I.S. and Jones, T.B. (1990) Biophys. J. 57, 173–182.
[12] Pohl, H.A. (1968) J. Electrochem. Soc. 115, 155c.
[13] Pethig, R. (1979) in Dielectric and Electronic Properties of Biological Materials, pp. 186–206, John Wiley & Sons, Chichester, UK.
[14] Zimmermann, U. (1982) Biochim. Biophys. Acta 694, 227–277.
[15] Jones, T.B. (1986) J. Electrostat. 18, 55–62.
[16] Mognaschi, E.R. and Savini, A. (1983) J. Phys. D. Applied Phys. 16, 1533–1541.
[17] Jones, T.B. (1984) Proc. IEEE – Industry Applications Society 1984 Annual Meeting, Chicago, October, pp. 1136–1141.
[18] Pauly, H. and Schwan, H.P. (1966) Z. Naturforsch. 14b, 125–131.
[19] Fricke, H. and Curtis, H.J. (1935) Nature 135, 436.
[20] Fricke, H. and Morse, S. (1925) J. Gen. Physiol. 9, 153–167.
[21] Coster, H.G.L. and Smith, J.R. (1974) Biochim. Biophys. Acta 373, 151–164.
[22] Sher, L.D. (1968) Nature 220, 695–696.
[23] Maxwell, J.C. (1892) A Treatise on Electricity and Magnetism, 3rd Edn., Art. 310–314, Oxford University Press, London.
[24] Huang, Y., Holzel, R., Pethig, R. and Wang, X. (1992) Phys. Med. Biol. 37, 1499–1517.